doi:10.1038/nature08123

LETTERS

Cyclic AMP intoxication of macrophages by a *Mycobacterium tuberculosis* adenylate cyclase

Nisheeth Agarwal[1], Gyanu Lamichhane[1], Radhika Gupta[1], Scott Nolan[1] & William R. Bishai[1]

With 8.9 million new cases and 1.7 million deaths per year, tuberculosis is a leading global killer that has not been effectively controlled[1,2]. The causative agent, *Mycobacterium tuberculosis*, proliferates within host macrophages where it modifies both its intracellular and local tissue environment, resulting in caseous granulomas with incomplete bacterial sterilization[3,4]. Although infection by various mycobacterial species produces a cyclic AMP burst within macrophages that influences cell signalling, the underlying mechanism for the cAMP burst remains unclear[5–7]. Here we show that among the 17 adenylate cyclase genes present in *M. tuberculosis*, at least one (*Rv0386*) is required for virulence. Furthermore, we demonstrate that the Rv0386 adenylate cyclase facilitates delivery of bacterial-derived cAMP into the macrophage cytoplasm. Loss of Rv0386 and the intramacrophage cAMP it delivers results in reductions in TNF-α production via the protein kinase A and cAMP response-element-binding protein pathway, decreased immunopathology in animal tissues, and diminished bacterial survival. Direct intoxication of host cells by bacterial-derived cAMP may enable *M. tuberculosis* to modify both its intracellular and tissue environments to facilitate its long-term survival.

Bacterial pathogens have evolved highly specific mechanisms to proliferate in the host during infection. A common strategy is subversion of host cell signal transduction by the introduction of enzymes that modulate the levels of secondary messengers such as cAMP[8,9]. Macrophages produce intracellular cAMP through G-protein-coupled receptor (GPCR)-adenylate cyclases (ACs)[10]. Increased cAMP stimulates protein kinase A (PKA), leading to the phosphorylation of cAMP response-element-binding protein (CREB), and subsequent transcriptional changes including modulation of cytokine expression[11,12].

To survive intracellularly, *M. tuberculosis* inhibits the host phagosome maturation process that is bactericidal for other organisms[13] using mechanisms that are incompletely understood, but may include secreted proteins, lipids or polysaccharides[14–16]. At the tissue level, *M. tuberculosis* elicits an immune response that results in caseous necrosis and the formation of solid granulomas[17]. These lesions, which are avascular and possibly hypoxic, may allow chronic contained infection[18–20].

The *M. tuberculosis* CDC1551 genome reveals 17 genes containing class III adenylate cyclase domains, a feature shared by pathogenic mycobacteria such as *Mycobacterium avium* (12 adenylate cyclases) and *Mycobacterium marinum* (31 adenylate cyclases). In contrast, *Escherichia coli*, *Pseudomonas aeruginosa*, *Corynebacterium glutamicum* and *Streptomyces coelicolor* only have one adenylate cyclase[21]. Although a member of the *M. tuberculosis* complex, *Mycobacterium microti*, has been reported to block phagosome maturation by cAMP production within macrophages[7], the source and effects of cAMP during macrophage infection by mycobacteria remain unclear.

We observed that after a brief exposure to *M. tuberculosis*, J774 macrophage-like cells produced an intracellular cAMP burst, as previously reported with *M. tuberculosis* and other mycobacteria[5–7], which was ~threefold above baseline within 3 h (Fig. 1a). The cAMP burst, which is sustained for more than 16 h after infection, correlated with CREB phosphorylation in a dose-dependent manner (Fig. 1b), suggesting stimulation of the PKA–CREB pathway by cAMP. These responses were not increased above baseline in macrophages infected with heat-killed bacteria, indicating that live tubercle bacilli are required (Fig. 1c, d). Similar results were observed with human THP-1 macrophages (data not shown).

Because several signal transduction pathways may stimulate CREB phosphorylation, we evaluated CREB responses in the

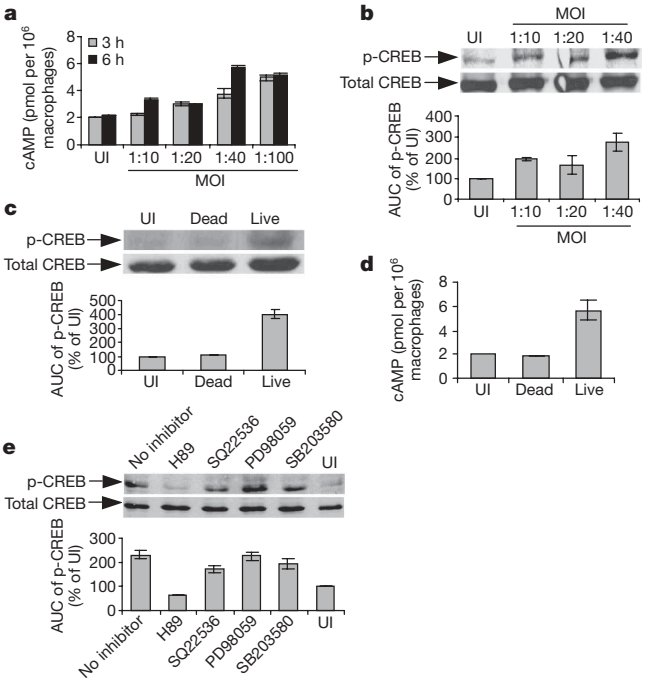

Figure 1 | The *M. tuberculosis*-induced macrophage cAMP burst and CREB phosphorylation pathway require live bacilli but not host GPCR-AC. **a**, **b**, Intramacrophage cAMP levels in J774 cells after 3 or 6 h (**a**) and CREB-phosphorylation (p-CREB) after 16 h compared with uninfected (UI) cells (**b**), at several multiplicities of infection (MOIs). AUC, area under the curve of the densitometric scan. **c**, **d**, Dead (heat-killed) bacilli fail to produce a p-CREB response at 16 h (**c**) or a cAMP burst at 3 h (**d**) in J774 cells. **e**, Sixteen hour p-CREB accumulation after *M. tuberculosis* infection requires PKA, as shown using the inhibitor H89, but is not dependent on host GPCR-AC, as shown using the inhibitor SQ22536 (see Methods, text and Fig. 4e for details about other inhibitors). Data are mean ± s.d. of multiple experiments ($n = 2$ in **b**, **c**, **e** and $n = 3$ in **a**, **d**).

[1]Department of Medicine, Johns Hopkins School of Medicine, CRB2, Room 1.08, 1550 Orleans Street, Baltimore, Maryland 21231-1044, USA.

M. tuberculosis-infected macrophages using specific pharmacological inhibitors against pathways involving ERK1/2 (PD98059), p38 MAPK (SB203580), or PKA (H89). As seen in Fig. 1e, *M. tuberculosis*-stimulated CREB phosphorylation was inhibited by less than 15% by PD98059 or SB203580 despite the fact that control immunoblots showed sustained inhibition of the targeted MAPKs over the incubation period. In contrast, H89 uniquely blocked infection-induced CREB phosphorylation by >70%, indicating a need for PKA activation; similar results were observed with an independent PKA inhibitor (Supplementary Fig. 1). Next we tested the inhibition of host cell GPCR-AC using SQ22536. Surprisingly, despite exposure to concentrations of SQ22536 that completely blocked forskolin-stimulated host cell adenylate cyclase activity, only partial inhibition of *M. tuberculosis*-induced CREB phosphorylation was observed with this inhibitor (Fig. 1e). Also, GPCR-AC inhibition by SQ22536 did not reduce cAMP levels in *M. tuberculosis*-infected cells. These findings indicated that endogenous macrophage GPCR-AC (the presumed source of cAMP and subsequent PKA activation) was not required for *M. tuberculosis*-induced CREB phosphorylation, and thus suggested that there might be an alternative source of cAMP.

To address the possibility that a bacterial adenylate cyclase might contribute to the intramacrophage cAMP burst[7], we measured cAMP production by *M. tuberculosis* in broth cultures and found notable levels both in the intracellular and extracellular compartments (Fig. 2a). Next, we constructed a recombinant *M. tuberculosis* strain overexpressing its endogenous phosphodiesterase (PDE) *Rv0805* (Mtb-PDE), and a corresponding empty-vector-containing control strain (Mtb-control). As detailed in the Methods, PCR with reverse transcription (RT–PCR) experiments confirmed an 8–12-fold overexpression of *Rv0805* in the Mtb-PDE strain compared to the Mtb-control strain. As predicted, overexpression of *Rv0805* significantly reduced intrabacterial cAMP both at early and late *in vitro* growth time points (Fig. 2b). Infection of macrophages with the Mtb-PDE strain showed that the overexpression of bacterial PDE—which is not secreted (Supplementary Fig. 2) and does not possess a signal sequence or lipid-anchoring domain, suggesting export—significantly reduced intramacrophage cAMP concentrations (Fig. 2c) as well as CREB phosphorylation (Fig. 2d) in comparison to the Mtb-control strain. In light of the observation that *M. avium*-stimulated CREB phosphorylation results in tumour necrosis factor-α (TNF-α) secretion[6], we also tested levels of TNF-α secretion by macrophages infected with the recombinant strains. As shown in Fig. 2e, infection with the Mtb-PDE strain resulted in ~fourfold less TNF-α secretion than with the Mtb-control strain. These results indicated that overexpression of a bacterial phosphodiesterase reduced intramacrophage cAMP levels as well as PKA-dependent events influenced by cAMP.

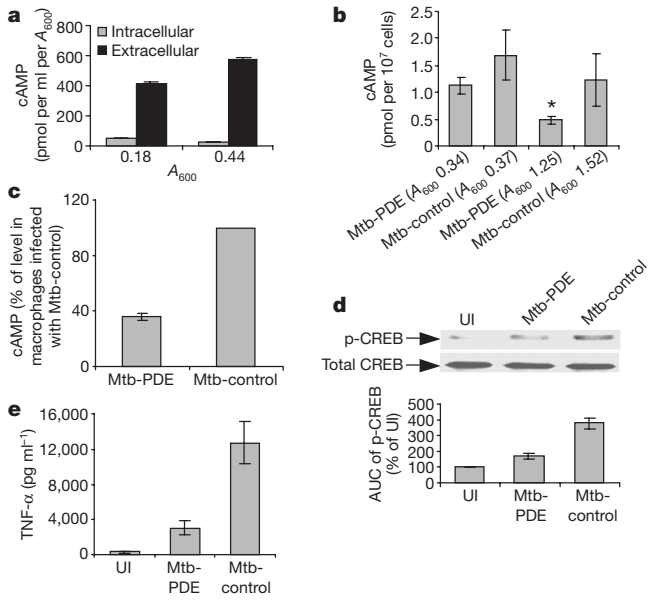

Figure 2 | Overexpression of phosphodiesterase *Rv0805* in *M. tuberculosis* reduces intramacrophage cAMP levels, CREB phosphorylation, and TNF-α secretion in infected J774 cells. **a**, **b**, *In vitro* cultures of *M. tuberculosis* secrete cAMP in the extracellular culture medium (**a**), and the Mtb-PDE strain shows reduced intrabacterial cAMP levels relative to the Mtb-control in early (A_{600} ~0.35) and late (A_{600} > 1.25) growth phases (**b**). **c**–**e**, Compared with the Mtb-control, Mtb-PDE-infected J774 cells show reduced intramacrophage cAMP levels (**c**), reduced CREB phosphorylation (**d**), and reduced TNF-α secretion (**e**). UI, uninfected. Data are mean ± s.d. of multiple experiments ($n = 2$ in **d** and $n = 3$ in **a**–**c**, **e**). *$P < 0.05$, two-tailed Student's *t* test.

To investigate the role of *M. tuberculosis* adenylate cyclases in pathogenesis further, we studied eight *M. tuberculosis* mutants each with a transposon insertion in a unique adenylate cyclase gene (Supplementary Fig. 3)[22]. Mice were infected with a pooled inoculum containing each of the adenylate cyclase mutants plus a control transposon mutant, JHU-1864c, known to be attenuated for survival in mice. Lung homogenates from groups of mice killed at four time points were plated, and the recovered pooled colonies were used to prepare *M. tuberculosis* genomic DNA for quantitative PCR using mutant-specific primers (Supplementary Table 1) to evaluate the relative abundance of each mutant (Supplementary Fig. 4). One of the eight mutants competing for survival in mouse lungs—the mutant in *Rv0386* (JHU-0386), which encodes a cell-wall associated adenylate cyclase (Supplementary Fig. 5)—showed a pattern of survival decline over time similar to that of the known attenuated strain JHU-1864c (Fig. 3a). To confirm this observation, we complemented the *Rv0386* mutation (JHU-0386 COMP, Supplementary Fig. 6), and infected three strains of mice (BALB/c, C57BL/6 and C57BL/6 mice lacking the *Tnfa* gene (C57BL/6 *Tnfa*$^{-/-}$)) by the aerosol route with the wild type, mutant, and complemented *M. tuberculosis* strains. As seen in Fig. 3b, the JHU-0386 mutant was significantly impaired for lung survival at late time points in immunocompetent mice (1.2 and 0.8 log units lower than wild type in BALB/c (at day 56) and in C57BL/6 (at day 28), respectively, $P < 0.05$ in both cases) and for dissemination to the spleen. In contrast, in mice lacking *Tnfa*, mutant and control strain proliferation was equivalent, indicating that the survival defect of JHU-0386 is dependent on host cell TNF-α.

We then tested macrophage cAMP levels with the *M. tuberculosis* mutant lacking the adenylate cyclase gene *Rv0386*. Infection with this mutant (which has an equivalent growth rate to wild type *in vitro* (data not shown) and in macrophages (Supplementary Fig. 7)), resulted in cAMP levels that were ~fivefold lower than those observed with wild-type *M. tuberculosis* (Fig. 3c). Similar results were observed in primary mouse macrophages (Supplementary Fig. 8a); moreover, the other seven adenylate cyclase mutants in the study failed to show an effect on intramacrophage cAMP levels (Supplementary Fig. 9). Providing an intact copy of the *Rv0386* gene to the JHU-0386 mutant by complementation restored intramacrophage cAMP levels to their wild-type levels, whereas complementation with a gene containing site-directed mutations producing two inactivating missense substitutions, N120Y and R124S, in the adenylate cyclase domain of Rv0386 (JHU-0386 SDM-COMP) failed to restore the cAMP burst (Fig. 3c) despite being expressed at comparable levels to wild-type *Rv0386* (data not shown). Furthermore, loss or restoration of the *Rv0386* gene did not influence macrophage cGMP levels (Supplementary Fig. 10). These data show that *Rv0386* is required for full virulence in the mouse model. Notably, loss of this adenylate cyclase gene results in a macrophage infection that is devoid of a cAMP burst. Taken together and in the context of the SQ22536 inhibition studies and the phosphodiesterase overexpression experiment, our data indicate that *M. tuberculosis*-derived cAMP contributes to the macrophage cAMP burst and implicate the bacterial adenylate cyclase Rv0386 in this process.

To investigate how the *M. tuberculosis* pathogenesis program might benefit by increasing intramacrophage cAMP levels, we

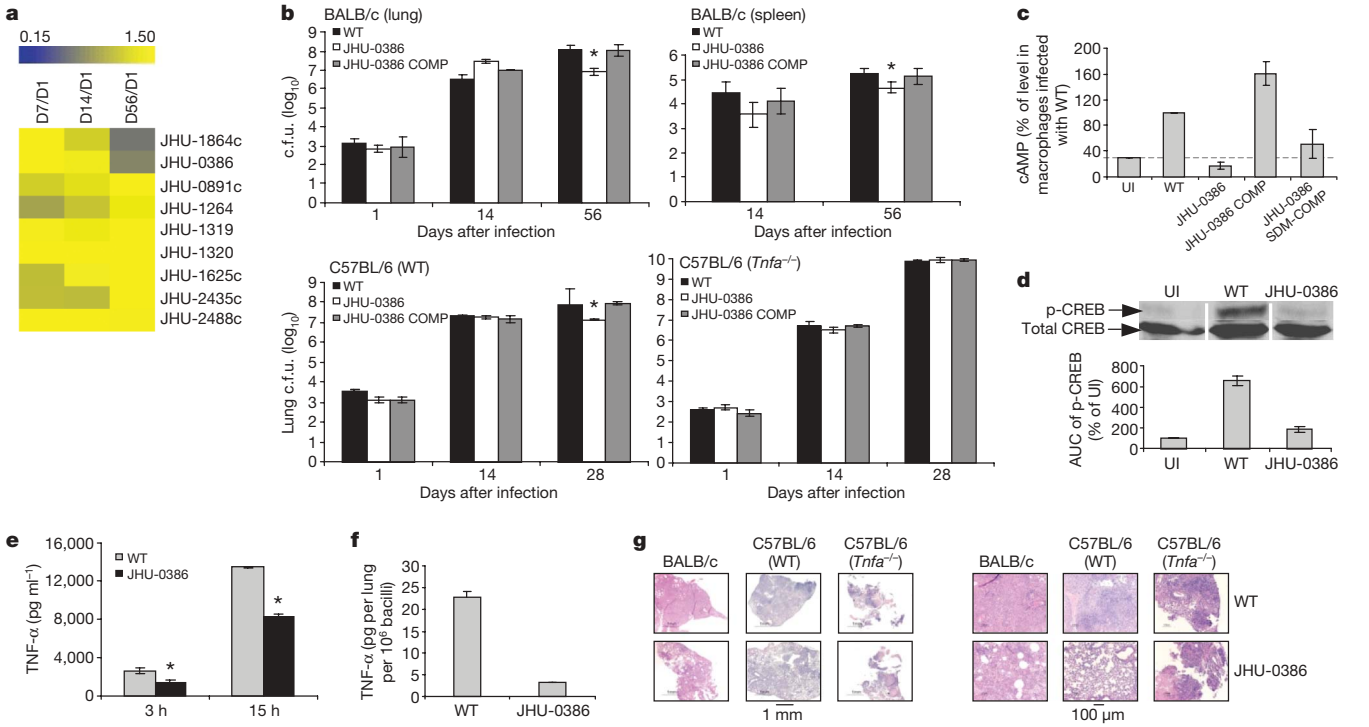

Figure 3 | The *M. tuberculosis Rv0386* mutant shows reduced mouse virulence, and lower levels of intramacrophage cAMP, CREB phosphorylation, and TNF-α secretion. **a**, Pooled mouse infection reveals that the *Rv0386* mutant shows a pattern of survival decline; colour intensity represents specific qPCR abundance relative to day 1 (D1). **b**, Single mutant infections show reduced *Rv0386* mutant survival at day 56 in BALB/c (top) and at day 28 in C57BL/6 (bottom left) mouse tissues, but not in *Tnfa*-deficient mice (bottom right). c.f.u., colony-forming units; WT, wild type. **c–e**, In J774 cells, the *Rv0386* mutant shows reduced intramacrophage cAMP levels at 3 h that are restored to wild-type levels by an intact complementing allele but not with site-directed mutations (SDM) in the adenylate cyclase domain (**c**). The mutant also shows reduced CREB-phosphorylation at 16 h (**d**), and reduced TNF-α secretion at the indicated times (**e**). **f**, **g**, Moreover, after aerosol infection, reduced TNF-α levels are seen in lung homogenates of JHU-0386-infected BALB/c mice at day 14 (**f**), and reduced cellular infiltration and airway loss at day 56 (BALB/c) or day 28 (C57BL/6), but no histological differences are seen at day 28 in *Tnfa*$^{-/-}$ C57BL/6 mice (**g**). Data are the mean values from several mice in **a** ($n = 4$), mean ± s.d. from multiple mice in **b**, **f** ($n = 3$), or mean ± s.d. of several experiments ($n = 2$ in **d**, $n = 3$ in **c**, **e**). *$P < 0.05$ between wild-type and JHU-0386 strains, by two-tailed Student's *t* test.

studied the signal transduction pathways during infection with the mutant lacking *Rv0386*. Macrophage infection by the *Rv0386* mutant elicited sharply reduced CREB phosphorylation signals, equivalent to levels in uninfected macrophages (Fig. 3d), and reduced TNF-α secretion, 40–50% below wild-type levels (Fig. 3e). To evaluate the impact of these *in vitro* reductions in inflammatory markers during whole animal infections, we evaluated TNF-α levels in BALB/c mouse lung homogenates following aerosol infection with wild type or the *Rv0386* mutant. As seen in Fig. 3f, lung TNF-α levels in the JHU-0386 mutant were nearly tenfold lower than those seen with the wild type. Concordantly, the histopathology of mouse lungs infected with the *Rv0386* mutant showed considerably less airway consolidation and inflammatory damage than the corresponding wild-type-infected tissues in both immunocompetent mouse strains (BALB/c and C57BL/6), but were equally severe in C57BL/6 *Tnfa*$^{-/-}$ mice (Fig. 3g).

To understand the mechanism of Rv0386 modulation of intramacrophage cAMP levels, we infected macrophages with *M. tuberculosis* strains pre-labelled with [^{14}C]-glycerol, and followed radiolabelled (bacterial-derived) cAMP levels using silica gel (Fig. 4a, b) or polyethylenimine (PEI) cellulose (Fig. 4c, d) thin-layer chromatography (TLC). There was a significant reduction in radiolabelled (bacterial-derived) cAMP levels by 60–80% in macrophages infected with the *Rv0386* mutant, but not in those infected with either the complemented *Rv0386* mutant or wild-type *M. tuberculosis* (Fig. 4b, d). These data indicate that cAMP derived from *M. tuberculosis* carbon pools enters macrophages after infection, and that loss of the *Rv0386* adenylate cyclase gene reduces the ability of *M. tuberculosis* to deliver bacterial-derived cAMP to the macrophage cytoplasm. On the basis of these findings, we propose that the Rv0386 gene product belongs to a mycobacterial cAMP generation and delivery system that produces cAMP within the host phagosome and facilitates its transport into the host cytoplasm, leading to excess cAMP and a subversion of cellular signal transduction (Fig. 4e).

Although several extracellular bacterial pathogens have evolved virulence effectors for modulating host cellular cAMP levels, either through G-protein modifying ADP ribosylation or secreted adenylate cyclase exotoxins (Fig. 4e)[23], subversion of host cell cAMP signal transduction by pathogenic mycobacteria has not been examined with modern tools. Our data indicate that the intracellular pathogen *M. tuberculosis* possesses at least one adenylate cyclase (Rv0386) that is required for the intramacrophage cAMP burst after phagocytosis, and that in the absence of *Rv0386*, CREB phosphorylation, TNF-α secretion, tissue immunopathology, and mouse virulence are reduced (Fig. 4e). The full consequences of cAMP intoxication of macrophages by *M. tuberculosis* are not fully determined and may include other pathways, such as host cell apoptosis[10,24].

Our data indicate that the microbe subverts the host cAMP signal transduction system to influence immune cell function, and that one consequence of this mechanism is early secretion of the pro-inflammatory cytokine TNF-α. A growing body of literature supports the concept of TNF-α dysregulation in the immunopathogenesis of tuberculosis. Indeed, low levels of TNF-α are well-known to be required for immune containment of latent *M. tuberculosis*[25,26], whereas in active disease high levels of TNF-α contribute to caseation necrosis, the blockade of dendritic cell maturation, and the development of granulomas that could serve the pathogen's purposes by providing an avascular sanctuary from cell-mediated immunity[27–29]. Although TNF-α secretion and granuloma formation are commonly

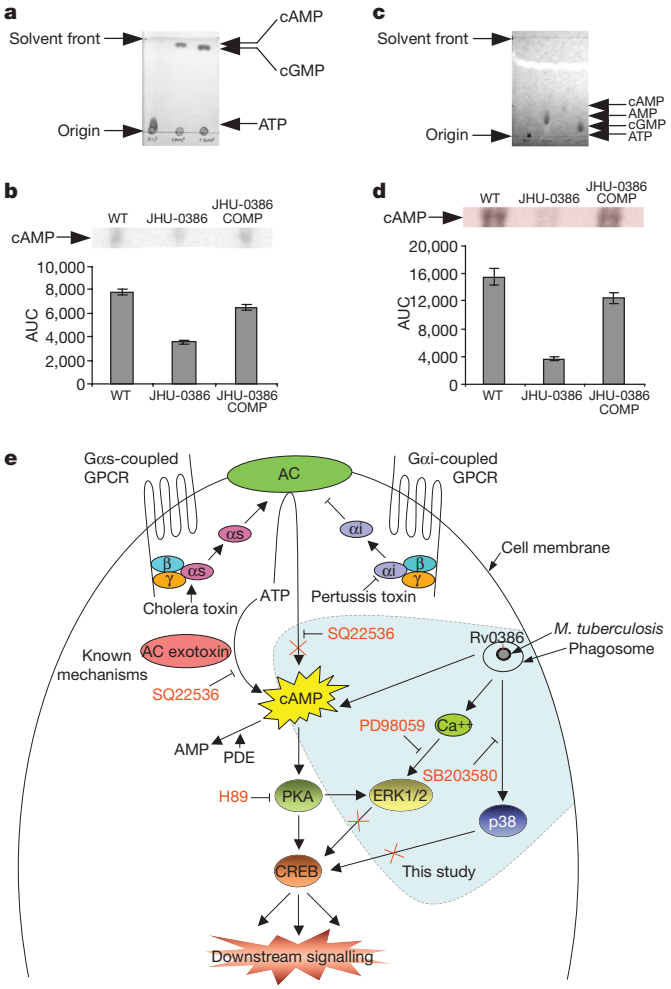

Figure 4 | Bacterial-derived cAMP enters the macrophage cytosol after infection. a, **c**, Silica gel TLC (**a**) and PEI cellulose chromatography (**c**) resolve the nucleotides indicated (ultraviolet visualization). **b**, **d**, After labelling *M. tuberculosis* strains with [^{14}C]-glycerol, J774 cells infected with the JHU-0386 mutant show significantly reduced bacterial-derived, radiolabelled cAMP in the intramacrophage compartment by silica gel TLC (**b**) or PEI cellulose separation (**d**) with autoradiography (top), and densitometric quantification (bottom). WT, wild type. Representative data of several experiments ($n = 2$ in **a**, **c**) or mean ± s.d. ($n = 2$ in **b**, **d**) are shown. **e**, Pathways of intracellular cAMP intoxication by pathogenic bacteria. This study shows that the *M. tuberculosis* adenylate cyclase Rv0386 is required for the infection-associated macrophage cAMP burst as well as CREB phosphorylation. Red crosses indicate pathways shown not to be involved in the infection-associated cAMP burst. See Supplementary Text 1 for details. AC, adenylate cyclase.

associated with mycobacterial containment, emerging evidence suggests that microbial growth and dissemination are paradoxically enhanced through host granuloma formation mechanisms. Recently, for example, granuloma formation was found to enhance both bacterial growth and dissemination in a manner dependent on the bacterial *RD1* gene locus in the *M. marinum*–zebrafish model[30]. Our data with *M. tuberculosis* in macrophages and mice support and extend this concept by showing that *M. tuberculosis* uses cAMP secretion to induce host TNF-α production, and that this results in more extensive lung disease and improved bacterial survival in immunocompetent mice. These findings suggest that *M. tuberculosis* elicits granuloma formation as part of its survival program.

METHODS SUMMARY

A detailed description of the bacterial strains, plasmids and growth conditions is provided in the full Methods. The PDE-overexpressing plasmid was constructed by cloning the gene encoding the phosphodiesterase of *M. tuberculosis*, *Rv0805*, into the mycobacterial expression vector pSD5 under the control of the *hsp60* promoter. *M. tuberculosis* CDC1551 transformed with empty vector, pSD5-hsp60 (Mtb-control), was used as a control strain in the experiments involving Mtb-PDE. The JHU-0386 mutant strain was complemented with either a wild-type or a mutant *Rv0386* allele, called *SDMRv0386*, containing two missense mutations leading to N120Y and R124S substitutions in Rv0386. N120 and R124 are predicted active site residues for the adenylate cyclase domain of Rv0386, and their replacement destroys adenylate cyclase activity. Estimation of bacterial loads in mouse organs was performed by quantitative real-time PCR (qPCR) or by single-strain infection. For estimation by qPCR, a pool of *M. tuberculosis* mutants in 8 of the 17 adenylate cyclase genes was used to infect BALB/c mice by the aerosol route. Bacterial colonies obtained from lungs of four mice at different time points were used for the preparation of genomic DNA. Bacillary proliferation of a specific mutant strain in mice lungs over a period of 56 days after infection was estimated by comparing the fold-changes in the relative abundance of strain-specific PCR products in the pool at different days with its relative abundance in the genomic DNA pool at day 1 by performing 35-cycle qPCR experiments. Cyclic AMP levels in the intra- and extracellular compartments of *M. tuberculosis*, and in the cytoplasm of J774 macrophage-like cells infected with *M. tuberculosis*, were estimated by ELISA using the cAMP Enzyme Immunoassay kit (Assay Designs Inc.) and by silica gel 60 F_{254} (Sigma) or cellulose PEI-F TLC (J.T. Baker Inc.). The levels of TNF-α secreted into the culture medium by infected macrophages or in the lung homogenates of infected mice were measured using a mouse TNF-α ELISA kit. Total and phosphorylated CREB levels in the macrophages were determined by immunoblotting using the clarified macrophage lysates with the respective antibodies and the luminol reagent. A detailed description of these methods is provided in the full Methods.

Full Methods and any associated references are available in the online version of the paper at www.nature.com/nature.

Received 1 April; accepted 30 April 2009.
Published online 10 June 2009.

1. Dye, C. Global epidemiology of tuberculosis. *Lancet* **367,** 938–940 (2006).
2. Wright, A. *et al.* Epidemiology of antituberculosis drug resistance 2002–07: an updated analysis of the Global Project on Anti-Tuberculosis Drug Resistance Surveillance. *Lancet* doi:10.1016/S0140-6736(09)60331-7 (in the press).
3. Flannagan, R. S., Cosio, G. & Grinstein, S. Antimicrobial mechanisms of phagocytes and bacterial evasion strategies. *Nature Rev. Microbiol.* **7,** 355–366 (2009).
4. Dannenberg, A. M. Jr. Immunopathogenesis of pulmonary tuberculosis. *Hosp. Pract. (Off. Ed.)* **28,** 51–58 (1993).
5. Bai, G., Schaak, D. D. & McDonough, K. A. cAMP levels within *Mycobacterium tuberculosis* and *Mycobacterium bovis* BCG increase upon infection of macrophages. *FEMS Immunol. Med. Microbiol.* **55,** 68–73 (2009).
6. Roach, S. K., Lee, S. B. & Schorey, J. S. Differential activation of the transcription factor cyclic AMP response element binding protein (CREB) in macrophages following infection with pathogenic and nonpathogenic mycobacteria and role for CREB in tumor necrosis factor α production. *Infect. Immun.* **73,** 514–522 (2005).
7. Lowrie, D. B., Jackett, P. S. & Ratcliffe, N. A. *Mycobacterium microti* may protect itself from intracellular destruction by releasing cyclic AMP into phagosomes. *Nature* **254,** 600–602 (1975).
8. Baker, D. A. & Kelly, J. M. Structure, function and evolution of microbial adenylyl and guanylyl cyclases. *Mol. Microbiol.* **52,** 1229–1242 (2004).
9. Sands, W. A. & Palmer, T. M. Regulating gene transcription in response to cyclic AMP elevation. *Cell. Signal.* **20,** 460–466 (2008).
10. Serezani, C. H., Ballinger, M. N., Aronoff, D. M. & Peters-Golden, M. Cyclic AMP: master regulator of innate immune cell function. *Am. J. Respir. Cell Mol. Biol.* **39,** 127–132 (2008).
11. Johannessen, M. & Moens, U. Multisite phosphorylation of the cAMP response element-binding protein (CREB) by a diversity of protein kinases. *Front. Biosci.* **12,** 1814–1832 (2007).
12. Servillo, G., Della Fazia, M. A. & Sassone-Corsi, P. Coupling cAMP signaling to transcription in the liver: pivotal role of CREB and CREM. *Exp. Cell Res.* **275,** 143–154 (2002).
13. Pethe, K. *et al.* Isolation of *Mycobacterium tuberculosis* mutants defective in the arrest of phagosome maturation. *Proc. Natl Acad. Sci. USA* **101,** 13642–13647 (2004).
14. Walburger, A. *et al.* Protein kinase G from pathogenic mycobacteria promotes survival within macrophages. *Science* **304,** 1800–1804 (2004).
15. Fratti, R. A., Chua, J., Vergne, I. & Deretic, V. *Mycobacterium tuberculosis* glycosylated phosphatidylinositol causes phagosome maturation arrest. *Proc. Natl Acad. Sci. USA* **100,** 5437–5442 (2003).
16. Axelrod, S. *et al.* Delay of phagosome maturation by a mycobacterial lipid is reversed by nitric oxide. *Cell. Microbiol.* **10,** 1530–1545 (2008).
17. Hunter, R. L., Jagannath, C. & Actor, J. K. Pathology of postprimary tuberculosis in humans and mice: contradiction of long-held beliefs. *Tuberculosis (Edinb.)* **87,** 267–278 (2007).

18. Tsai, M. C. *et al.* Characterization of the tuberculous granuloma in murine and human lungs: cellular composition and relative tissue oxygen tension. *Cell. Microbiol.* **8,** 218–232 (2006).
19. Timm, J. *et al.* Differential expression of iron-, carbon-, and oxygen-responsive mycobacterial genes in the lungs of chronically infected mice and tuberculosis patients. *Proc. Natl Acad. Sci. USA* **100,** 14321–14326 (2003).
20. Via, L. E. *et al.* Tuberculous granulomas are hypoxic in guinea pigs, rabbits, and nonhuman primates. *Infect. Immun.* **76,** 2333–2340 (2008).
21. Shenoy, A. R., Sivakumar, K., Krupa, A., Srinivasan, N. & Visweswariah, S. S. A survey of nucleotide cyclases in Actinobacteria: unique domain organization and expansion of the class III cyclase family in *Mycobacterium tuberculosis*. *Comp. Funct. Genomics* **5,** 17–38 (2004).
22. Lamichhane, G. *et al.* A postgenomic method for predicting essential genes at subsaturation levels of mutagenesis: application to *Mycobacterium tuberculosis*. *Proc. Natl Acad. Sci. USA* **100,** 7213–7218 (2003).
23. Ahuja, N., Kumar, P. & Bhatnagar, R. The adenylate cyclase toxins. *Crit. Rev. Microbiol.* **30,** 187–196 (2004).
24. von Knethen, A. & Brune, B. Attenuation of macrophage apoptosis by the cAMP-signaling system. *Mol. Cell. Biochem.* **212,** 35–43 (2000).
25. Keane, J. *et al.* Tuberculosis associated with infliximab, a tumor necrosis factor α-neutralizing agent. *N. Engl. J. Med.* **345,** 1098–1104 (2001).
26. Chakravarty, S. D. *et al.* Tumor necrosis factor blockade in chronic murine tuberculosis enhances granulomatous inflammation and disorganizes granulomas in the lungs. *Infect. Immun.* **76,** 916–926 (2008).
27. Bekker, L. G. *et al.* Immunopathologic effects of tumor necrosis factor alpha in murine mycobacterial infection are dose dependent. *Infect. Immun.* **68,** 6954–6961 (2000).
28. Clay, H., Volkman, H. E. & Ramakrishnan, L. Tumor necrosis factor signaling mediates resistance to mycobacteria by inhibiting bacterial growth and macrophage death. *Immunity* **29,** 283–294 (2008).
29. Hanekom, W. A. *et al. Mycobacterium tuberculosis* inhibits maturation of human monocyte-derived dendritic cells *in vitro*. *J. Infect. Dis.* **188,** 257–266 (2003).
30. Davis, J. M. & Ramakrishnan, L. The role of the granuloma in expansion and dissemination of early tuberculous infection. *Cell* **136,** 37–49 (2009).

Supplementary Information is linked to the online version of the paper at www.nature.com/nature.

Acknowledgements The support of National Institutes of Health (NIH) awards AI30036, AI36973 and AI37856 is gratefully acknowledged.

Author Contributions N.A. and W.R.B. designed the research. N.A. performed the experiments. R.G., S.N. and G.L. designed and contributed to the mouse experiments. N.A. and W.R.B. analysed the data and wrote the paper.

Author Information Reprints and permissions information is available at www.nature.com/reprints. Correspondence and requests for materials should be addressed to W.R.B. (wbishai@jhmi.edu).

METHODS

Bacterial strains, plasmids and growth conditions. In this study we used *Escherichia coli* strain DH5α and *M. tuberculosis* CDC1551, as described earlier[31]. Details on the transposon insertion mutants of *M. tuberculosis* used in this study (Supplementary Fig. 3) may be found on the TARGET website of the Johns Hopkins University (http://webhost.nts.jhu.edu/target/). Plasmid pSD5-hsp60 (mycobacteria-*E. coli* shuttle vector for protein expression in *M. tuberculosis* from the strong mycobacterial promoter, P*hsp60*) was kindly provided by A. Tyagi, University of Delhi South Campus. Both *E. coli* and mycobacterial strains were grown as described[31] from frozen glycerol stocks stored at −70 °C. All reagents to grow mycobacteria were tested for the absence of endotoxin contamination using the E-Toxate assay (Sigma-Aldrich).

Overexpression of *Rv0805* in *M. tuberculosis*. The gene encoding the PDE of *M. tuberculosis*, *Rv0805* (ref. 32), was PCR-amplified from *M. tuberculosis* chromosomal DNA using gene-specific primers, PrRv0805(F) and PrRv0805(R) (Supplementary Table 1), using conditions described earlier[32]. The amplicons were cloned into the mycobacterial expression vector pSD5-hsp60 at the Nde I and PstI sites. The resulting construct pSD5-hsp60_Rv0805 was sequenced and subsequently used to transform *M. tuberculosis* CDC1551. Overexpression of *Rv0805* in the Mtb-PDE strain was confirmed by real-time RT–PCR as described previously[31], using *Rv0805*-specific primer pairs (Rv0805_RT(F) and Rv0805_RT(R); Supplementary Table 1). *M. tuberculosis* CDC1551 transformed with empty vector, pSD5-hsp60 (Mtb-control), was used as a control strain in the experiments involving Mtb-PDE. For overexpression of *Rv0805* fused with a C-terminal Flag tag, *Rv0805* was PCR amplified by using gene-specific primers, PrRv0805(F) and Rv0805Flag(R) (Supplementary Table 1), and cloned into the mycobacterial expression vector pSD5-hsp60 as described earlier.

Expression of *Rv0386*-Flag in *M. tuberculosis*. To express the *Rv0386* fused with the Flag tag at its C terminus in *M. tuberculosis*, a 3,762 base pair (bp) DNA fragment including the coding sequence of the *Rv0386* gene, 459 bp of 5′ sequence (including the gene's native promoter), and 24 bp of Flag sequence at the 3′ end was PCR-amplified with the primers pGWRv0386_F and pGWRv0386 (Flag)_R (Supplementary Table 1). Using the Gateway cloning system (Invitrogen), these amplicons were cloned into the destination vector pGS202R, which is a hygromycin resistance (Hyg^R) derivative of mycobacterial integrating vector pMH94 containing LR recombination sites (G.L. and S.N., unpublished data). The resulting construct, pGS202R-Rv0386-Flag, was subjected to nucleotide sequencing and subsequently used to transform *M. tuberculosis* CDC1551. Candidate Hyg^R colonies were selected, and the presence of the intact *Rv0386*-Flag gene was identified by PCR and Southern blotting.

Construction of *Rv0386* complementation strains. To complement the JHU-0386 mutant, a 3,738 bp DNA fragment including the coding sequence of the *Rv0386* gene and 459 bp of 5′ sequence (including the gene's native promoter) was amplified by PCR with primers pGWRv0386_F and pGWRv0386_R (Supplementary Table 1) and cloned into the destination vector, pGS202R, as described above. The resulting construct, pGS202R-Rv0386, was subjected to nucleotide sequencing and subsequently used to transform the *M. tuberculosis* JHU-0386 mutant strain which is kanamycin resistant (Kan^R). Candidate Hyg^R and Kan^R colonies were selected, and the presence of the intact complementing *Rv0386* allele was identified by PCR and Southern blotting. We also constructed a mutant complementing *Rv0386* allele, called SDMRv0386, which contains two missense mutations leading to N120Y and R124S substitutions in Rv0386. This was made with primer pairs pSDMRv0386_F and pSDMRv0386_R (Supplementary Table 1) together with pGS202R-Rv0386-Flag template DNA using QuikChange XL site-directed mutagenesis kit (Stratagene) according to the manufacturer's instructions. The resulting construct, pGS202R-SDMRv0386, was subjected to nucleotide sequencing and subsequently used to transform the *M. tuberculosis* JHU-0386 mutant strain.

Mycobacterial infection of mice and estimation of bacterial load by quantitative real-time PCR. A pool of *M. tuberculosis* mutants in 8 of 17 adenylate cyclase genes was used to infect BALB/c mice by the aerosol route, with an inoculum that implanted $\sim 3.7 \times 10^3$ c.f.u. in the lungs at day 1. Groups of four mice were killed at days 1, 7, 14 and 56 after infection, and the respective lung homogenates were plated on 7H11 agar medium to obtain mycobacterial colonies representing a heterogeneous population of different mutants residing in mouse lungs at each time point. Bacterial colonies obtained from lungs of four mice at each time point were scraped from 7H11 agar plates, pooled, and used for preparation of genomic DNA. Genomic DNA was prepared from pooled mycobacterial colonies, quantified by measuring absorbance at 260 nm, and used for quantitative real-time PCR (qPCR) experiments. Bacterial proliferation of specific mutant strains in mouse lungs over a period of 56 days after infection was estimated by comparing fold-changes in the relative abundance of each strain-specific PCR product in the pool at different days with their relative abundance in the genomic DNA pool at day 1 by performing 35-cycle qPCR experiments. Each qPCR experiment was performed using 10 ng of genomic DNA prepared from the pooled mycobacterial colonies obtained from mouse lungs at each of the time points (day 1 and the following days), and a primer pair (containing transposon-specific primer SP1, and an adenylate-cyclase-specific primer; Supplementary Table 1) designed to amplify ~200 bp junctional DNA sequences specific for the transposon point of insertion of each adenylate cyclase mutant (Supplementary Fig. 3). Fold-changes in relative abundance of mutant-specific DNA were measured by normalizing PCR product abundance to that of *sigA*. qPCR values for a particular time point were normalized to that for day 1. Ratio values lower than one indicate reduced survival in the mouse lung at that time point.

Infection of mice with single mycobacterial strains. Single strain infections of 4–5-week-old BALB/c or C57BL/6 mice and 4–7-week-old *Tnfa*-deficient mice, 129S6-*Tnf*^{tm1Gkl}/J, were performed with the JHU-0386, wild-type CDC1551 and JHU-0386 COMP strains of *M. tuberculosis* by the aerosol route, with an inoculum that implanted $\sim 10^3$ c.f.u. in the lungs of BALB/c or C57BL/6 and $\sim 10^2$ c.f.u. in the lungs of *Tnfa*-deficient mice, respectively, at day 1. Three mice from each group were subsequently killed at day 1 and weeks 2, 4 and 8 post-infection to determine the organ c.f.u. counts. Lung and spleen tissues were homogenized in their entirety in PBS, and colonies were enumerated on selective 7H11 plates after 3 weeks of incubation at 37 °C.

Infection of macrophages with *M. tuberculosis*. Infection ratios were determined by fluorescence microscopy; live or heat-killed mycobacteria were tagged with Sulfo-NHS-Biotin (Pierce) and subsequently used for infection of J774 macrophage-like cells. For 3 h infections, macrophages were incubated with the inoculating mycobacterial suspension in RPMI for 3 h, followed by three washes with PBS; for 6 h infections, macrophages were incubated for a further 3 h after PBS washes. At the end of the infection at each time point, macrophages were fixed on coverslips and incubated with DyLight-488-conjugated streptavidin in 1% BSA, 0.1% saponin in PBS for 4 h. Fluorescent mycobacterial cells were visualized using fluorescent microscopy, and the level of infection was quantified by counting the number of cells infected in at least five fields per replicate. No fewer than 100 cells per replicate were counted. Macrophages infected with a 1:40 MOI for 3 h resulted in ~70–80% of cells infected, and those with a 1:40 MOI for 6 h resulted in >85% of cells infected; cell viability remained >75% under all conditions as estimated by trypan blue staining. For infection of primary macrophages, bone marrow derived macrophages were isolated from 5–7-week-old BALB/c mice as described earlier[6].

ELISA. For estimation of intramacrophage cAMP or cGMP levels, macrophages were seeded on 6-well plates at 5×10^5 cells per well for 24 h, and infected with mycobacteria for 3 h with a 1:40 MOI as described earlier before lysis. ELISAs were performed with the macrophage lysates by using Enzyme Immunoassay Kits (Assay Designs Inc.) according to the manufacturer's instructions. Intrabacterial cAMP levels in *M. tuberculosis* were estimated by generating a clarified bacterial lysate after heat lysis of bacterial suspensions in 0.1 M HCl. Prior to acid-heat lysis, dilutions of this suspension were spread on 7H11 agar plates for bacterial enumeration, and the intrabacterial cAMP levels in *M. tuberculosis* were estimated as pmol per 10^7 bacilli. Levels of TNF-α secreted into the culture medium by infected macrophages (MOI 1:100 for 3 h), or in lung homogenates of infected mice, were measured using the R&D Systems Quantikine Mouse TNF-α/TNFSF1A Immunoassay ELISA kit. For estimation of TNF-α in mouse lungs infected with a particular bacterial strain, equal volumes of lung homogenates from three infected mice were combined and used for TNF-α measurement.

***M. tuberculosis* cell lysate preparation.** *M. tuberculosis* cell lysates were prepared from mid-log-phase cultures in PBS by bead-beating followed by centrifugation at high speed for 10 min. The pellet fraction comprising cell envelop proteins was subsequently washed twice with PBS, suspended in SDS loading dye, and boiled for 5 min. The supernatant fraction corresponding to cytosolic proteins was passed through a 0.22 μm filter, mixed with SDS loading dye, and boiled for 5 min. For SDS–PAGE, equal amount of proteins from both the fractions were loaded onto SDS–PAGE gels.

Western blot analysis. Macrophages were seeded on 6-well plates at 5×10^5 cells per well, and 24 h later were infected with mycobacteria with a 1:40 MOI for 3 h, and subsequently subjected to three washes with PBS. Infections were then allowed to progress for 13 h. Total CREB or phosphorylated CREB western immunoreactivity of macrophage lysates was performed as described[6]. Levels of p-CREB were quantified by densitometry of anti-phosphorylated-CREB immunoblots from at least two independent experiments, and the values were obtained after normalization to the respective total CREB intensities. Anti-Flag western immunoreactivity of mycobacterial cell lysates was performed according to the manufacturer's instructions (Sigma).

Detection of cAMP in infected J774 macrophage-like cells by TLC. *M. tuberculosis* cell pellets were suspended in PBS containing 0.02% Tween-80 (PBS-T) and incubated with 1 μCi ml^{-1} of [^{14}C]-glycerol at 37 °C with shaking for 4 h. Subsequently, cells were pelleted, washed with PBS and suspended in complete 7H9 medium for overnight growth at 37 °C. The next day, before infection, the labelled mycobacterial cell pellets were washed twice with PBS-T and suspended in RPMI. J774 macrophage-like cells were infected with radiolabelled mycobacteria with a 1:40 MOI for 3 h as described above. At the end of the infection, macrophages were lysed in 0.1 M HCl plus 0.05% Triton X-100 for 15 min on ice. The cell debris was separated by centrifugation at high speed, and the protein concentration in the lysate was estimated using Bradford's reagent. For comparisons between different samples, lysate volumes were adjusted for protein concentration, and equal protein amounts were spotted on the thin layer medium. Before spotting, lysate proteins were precipitated by boiling for 1 min in a dry block; after centrifugation at high speed, the supernatant was spotted on either Silica gel 60 F_{254} (Sigma) or Cellulose PEI-F (J.T. Baker Inc.) TLC sheets (20 × 10 cm). Ascending chromatography was conducted for 1 h at room temperature (25 °C)[33,34]. Commercially available purified nucleotides were spotted alongside the samples to identify the position of cAMP and other nucleotides. Separated nucleotides were visualized with short-wave ultraviolet light. Radiolabelled cAMP fractions were visualized by autoradiography with a PhosphorImager (Molecular Dynamics).

Inhibitor treatment. The inhibitors were purchased from Calbiochem, reconstituted either in sterile, endotoxin-tested water or dimethylsulphoxide (DMSO) according to manufacturer's recommendations, and used at the following concentrations: H89 (50 μM), SQ22536 (200 μM), PD98059 (50 μM) and SB203580 (50 μM). DMSO was used at the same concentrations as the vehicle control. Another PKA-specific inhibitor, protein kinase A inhibitor fragment 14-22, myristoylated trifluoroacetate salt (PKA-I) was purchased from Sigma and used at 40 μM. Macrophages were treated with these inhibitors or DMSO 1 h before infection. For all inhibitors, a dose-response relationship was observed in relation to CREB phosphorylation (for H89 or SQ22536), ERK1/2 phosphorylation (for PD98059), or p38 phosphorylation (for SB203580) (data not shown), and the concentrations used in subsequent studies were chosen on the basis of the dose-response curve. None of the inhibitors used had a significant effect on macrophage uptake of mycobacteria.

Statistical analysis. Statistical significance was determined with the paired two-tailed Student's *t* test at $P < 0.05$ level of significance using InStat/Prism software.

31. Agarwal, N., Woolwine, S. C., Tyagi, S. & Bishai, W. R. Characterization of the *Mycobacterium tuberculosis* sigma factor SigM by assessment of virulence and identification of SigM-dependent genes. *Infect. Immun.* **75,** 452–461 (2007).
32. Shenoy, A. R., Sreenath, N., Podobnik, M., Kovacevic, M. & Visweswariah, S. S. The Rv0805 gene from *Mycobacterium tuberculosis* encodes a 3′,5′-cyclic nucleotide phosphodiesterase: biochemical and mutational analysis. *Biochemistry* **44,** 15695–15704 (2005).
33. Higashida, H., Hossain, K. Z., Takahagi, H. & Noda, M. Measurement of adenylyl cyclase by separating cyclic AMP on silica gel thin-layer chromatography. *Anal. Biochem.* **308,** 106–111 (2002).
34. Böhme, E. & Schultz, G. Separation of cyclic nucleotides by thin-layer chromatography on polyethyleneimine cellulose. *Methods Enzymol.* **38,** 27–38 (1974).